

$SU(2)$ lattice gluon propagators at finite temperatures in the deep infrared region and Gribov copy effects

V. G. Bornyakov

*High Energy Physics Institute, Protvino, Russia
and Institute of Theoretical and Experimental Physics, 117259 Moscow, Russia*

V. K. Mitrjushkin

*Joint Institute for Nuclear Research, 141980 Dubna, Russia
and Institute of Theoretical and Experimental Physics, 117259 Moscow, Russia*

We study numerically the $SU(2)$ Landau gauge transverse and longitudinal gluon propagators at non-zero temperatures T both in confinement and deconfinement phases. The special attention is paid to the Gribov copy effects in the IR-region. Applying powerful gauge fixing algorithm we find that the Gribov copy effects for the transverse propagator $D_T(p)$ are very strong in the infrared, while the longitudinal propagator $D_L(p)$ shows very weak (if any) Gribov copy dependence. The value $D_T(0)$ tends to decrease with growing lattice size; however, $D_T(0)$ is *non-zero* in the infinite volume limit, in disagreement with the suggestion made in [1]. We show that in the infrared region $D_T(p)$ is not consistent with the pole-type formula *not only* in the deconfinement phase but also for $T < T_c$. We introduce new definition of the magnetic infrared mass scale ('magnetic screening mass') m_M . The electric mass m_E has been determined from the momentum space longitudinal gluon propagator. We study also the (finite) volume and temperature dependence of the propagators as well as discretization errors.

PACS numbers: 11.15.Ha, 12.38.Gc, 12.38.Aw

Keywords: Lattice gauge theory, gluon propagator, finite temperature, Gribov problem, simulated annealing

I. INTRODUCTION

One of the most interesting features of the quantum chromodynamics at finite temperature is the transition from the confinement to the deconfinement phase. This transition separates a low-temperature phase, which is expected to be highly non-perturbative and characterized by quark and gluon confinement, from a high-temperature - quark-gluon plasma (QGP) - phase, where color charges should be deconfined. The conjecture of the existence of the QGP has been supported by recent observations of the collective effects in ultrarelativistic heavy-ion collisions at SPS and RHIC (see, e.g., [2] and references therein).

The non-perturbative - first principle - calculation of gauge variant gluon (as well as ghost) propagators is of interest for various reasons. These propagators are expected to show different behavior in each phase and, therefore, to serve as a useful 'order parameters', detecting the phase transition point T_c . One expects that their study can shed the light on the mechanism of the confinement-deconfinement transition. Another reason is that for the reliable phenomenological analysis of high-energy heavy-ion collision data, it is important to obtain information on the momentum dependence of the longitudinal (electric) gluon propagator $D_L(p)$ and transverse (magnetic) gluon propagator $D_T(p)$, especially in the (deep) infrared region. One example is the study of the radiative energy loss in dense nuclear matter (jet quenching) which results from the energy loss of high energy partons moving

through the plasma (see, e.g., [3–7]). Also, the non-perturbatively calculated lattice propagators are to be used to check the correctness of various analytical methods in QCD, e.g., Dyson–Schwinger equations (DSE) method. For study of the gluon propagator using DSE approach at finite temperature see e.g. [8–10].

The lattice study of the finite temperature $SU(2)$ gluon propagators in Landau gauge has been performed in a number of papers (see, e.g., papers [10–15]). In Ref. [13] the electric and magnetic propagators were studied in both coordinate and momentum spaces and in 4 and 3 dimensions. The conclusion was made that the magnetic propagator had a complicated infrared behavior which was not compatible with simple pole mass behavior. It was also found that this propagator had strong volume and gauge dependence. In Refs. [10, 15] results for both gluon and ghost propagators in momentum space were presented, but some important questions, e.g. Gribov copies effects, infrared behavior and scaling were not addressed.

In paper [1] it has been suggested that the proximity of the Gribov horizon at finite temperature forces the transverse gluon propagator $D_T(\vec{p}, p_4 = 0)$ to vanish at zero three-momentum. If this is the case, then the finite-temperature analog of Gribov formula $|\vec{p}|^2 / (|\vec{p}|^4 + M_M^4) \equiv 1 / (|\vec{p}|^2 + m_{eff}^2(\vec{p}))$ suggests that the *effective* magnetic screening mass $m_{eff}(\vec{p})$ becomes infinite in the infrared (interpreted as a magnetic gluons 'confinement').

The Gribov copy effects still remain one of the most

serious problem in the lattice calculations, at least, in the deep IR-region. In our study we employ the gauge condition which requires the Landau gauge fixing functional F (see the definition in Section II) to take extrema as close as possible to the *global* extremum. This choice for the gauge condition is supported by the following facts: **a)** a consistent non-perturbative gauge fixing procedure proposed by Parrinello-Jona-Lasinio and Zwanziger (PJLZ-approach) [16, 17] presumes that the choice of a unique representative of the gauge orbit should be through the *global* extremum of the chosen gauge fixing functional; **b)** in the case of pure gauge $U(1)$ theory in the weak coupling (Coulomb) phase some of the gauge copies produce a photon propagator with a decay behavior inconsistent with the expected zero mass behavior [18–20]. The choice of the global extremum permits to obtain the physical - massless - photon propagator.

In a series of papers [21–25] we investigated the Gribov copy effects in the Landau gauge gluon (and/or ghost) propagators in zero temperature $SU(2)$ gluodynamics. It has been demonstrated unambiguously that these effects are *strong* in the infrared¹. Thus the Gribov copy effects reduction is very important for the infrared behavior studies. Recently it has been pointed out in Ref. [26] that lattice results for the infrared gluon and ghost propagators free of Gribov copies effects would help to discriminate between scaling and decoupling solutions of the Dyson-Schwinger equations. In this paper we undertake a careful study of the Gribov copy effects in the Landau gauge gluon propagator at finite temperature. We employ the gauge fixing procedure which we used recently in our study at zero temperature [25] with changes dictated by nonzero temperature (see Section III).

Also we attempt to make a careful analysis of (finite) volume and temperature dependence of D_T and D_L as well as of scaling violations.

Section II contains main definitions as well as some details of simulations and gauge fixing procedure we use. Section III is dedicated to the study of the Gribov copy effects. Volume and temperature dependence of the propagators as well as discretization errors are discussed in Section IV. Section V is dedicated to the discussion of the screening masses and Section VI is reserved for conclusions and discussion.

II. GLUON PROPAGATORS: THE DEFINITIONS

We study the $SU(2)$ lattice gauge theory with the standard Wilson action

$$S = \beta \sum_x \sum_{\mu > \nu} \left[1 - \frac{1}{2} \text{Tr} \left(U_{x\mu} U_{x+\mu;\nu} U_{x+\nu;\mu}^\dagger U_{x\nu}^\dagger \right) \right],$$

where $\beta = 4/g_0^2$ and g_0 is a bare coupling constant. The link variables $U_{x\mu} \in SU(2)$ transform under gauge transformations g_x as follows:

$$U_{x\mu} \xrightarrow{g} U_{x\mu}^g = g_x^\dagger U_{x\mu} g_{x+\mu}; \quad g_x \in SU(2). \quad (1)$$

Our calculations were performed on the asymmetric lattices with lattice volume $V = L_4 \cdot L_s^3$, where L_4 is the number of sites in the 4th direction. The temperature T is given by

$$T = \frac{1}{aL_4}, \quad (2)$$

where a is the lattice spacing. We employ the standard definition of the lattice gauge vector potential $\mathcal{A}_{x+\hat{\mu}/2,\mu}$ [27]:

$$\mathcal{A}_{x+\hat{\mu}/2,\mu} = \frac{1}{2i} \left(U_{x\mu} - U_{x\mu}^\dagger \right) \equiv A_{x+\hat{\mu}/2,\mu}^a \frac{\sigma_a}{2}. \quad (3)$$

The Landau gauge fixing condition is

$$(\partial \mathcal{A})_x = \sum_{\mu=1}^4 (\mathcal{A}_{x+\hat{\mu}/2,\mu} - \mathcal{A}_{x-\hat{\mu}/2,\mu}) = 0, \quad (4)$$

which is equivalent to finding an extremum of the gauge functional

$$F_U(g) = \frac{1}{4V} \sum_{x\mu} \frac{1}{2} \text{Tr} U_{x\mu}^g, \quad (5)$$

with respect to gauge transformations g_x . After replacing $U \Rightarrow U^g$ at the extremum the gauge condition (4) is satisfied.

The (unrenormalized) gluon propagator $D_{\mu\nu}^{ab}(p)$ is defined as follows

$$D_{\mu\nu}^{ab}(p) = \frac{a^2}{g_0^2} \langle \tilde{A}_\mu^a(k) \tilde{A}_\nu^b(-k) \rangle$$

where $\tilde{A}(k)$ represents the Fourier transform of the gauge potentials defined in Eq.(3) after having fixed the gauge, $k_i \in (-L_s/2, L_s/2]$ and $k_4 \in$

¹ Unfortunately, authors of [15] cite our paper [22] in a completely misleading context.

$(-L_4/2, L_4/2]$. The physical momenta p_μ are given by $ap_i = 2 \sin(\pi k_i/L_s)$, $ap_4 = 2 \sin(\pi k_4/L_4)$.

In what follows we consider only *soft* modes $p_4 = 0$. The hard modes ($p_4 \neq 0$) have an *effective* thermal mass $2\pi T|k_4|$ and behave like massive particles².

As is well known, on the asymmetric lattice there are two tensor structures for the gluon propagator [28] :

$$D_{\mu\nu}^{ab}(p) = \delta_{ab} (P_{\mu\nu}^T(p) D_T(p) + P_{\mu\nu}^L(p) D_L(p)) , \quad (6)$$

where (symmetric) orthogonal projectors $P_{\mu\nu}^{T;L}(p)$ are defined at $p = (\vec{p} \neq 0; p_4 = 0)$ as follows

$$P_{ij}^T(p) = \left(\delta_{ij} - \frac{p_i p_j}{\vec{p}^2} \right), \quad P_{\mu 4}^T(p) = 0 ; \quad (7)$$

$$P_{44}^L(p) = 1 ; \quad P_{\mu i}^L(p) = 0 . \quad (8)$$

Therefore, two scalar propagators - longitudinal $D_L(p)$ and transverse $D_T(p)$ - are given by

$$\begin{aligned} D_T(p) &= \frac{1}{6} \sum_{a=1}^3 \sum_{i=1}^3 D_{ii}^{aa}(p) ; \\ D_L(p) &= \frac{1}{3} \sum_{a=1}^3 D_{44}^{aa}(p) , \end{aligned} \quad (9)$$

For $\vec{p} = 0$ propagators $D_T(0)$ and $D_L(0)$ are defined as follows

$$\begin{aligned} D_T(0) &= \frac{1}{9} \sum_{a=1}^3 \sum_{i=1}^3 D_{ii}^{aa}(0) , \\ D_L(0) &= \frac{1}{3} \sum_{a=1}^3 D_{00}^{aa}(0) . \end{aligned} \quad (10)$$

The transverse propagator $D_T(p)$ is associated to magnetic sector, and the longitudinal one $D_L(p)$ - to electric sector.

We generated ensembles of up to two thousand independent Monte Carlo lattice field configurations. Consecutive configurations (considered as independent) were separated by 100 (for $L_s < 32$) or 200 (for $L_s \geq 32$) sweeps, each sweep being of one local heat-bath update followed by $L_s/2$ microcanonical updates. In Table I we provide the full information about the field ensembles used throughout this paper.

In order to keep finite-volume effects under control, we considered a few different lattice volumes for each temperature. The choice of the 6×48^3 lattice at $\beta = 2.635$ is important for the check of the scaling behavior (see Section IV).

β	$a^{-1}[\text{Gev}]$	$a[\text{fm}]$	L_4	L_s	T/T_c	N_{meas}	N_{copy}
2.260	1.073	0.184	4	40	0.9	800	40
2.260	1.073	0.184	4	48	0.9	800	40
2.300	1.192	0.165	4	26	1.0	1200	24
2.300	1.192	0.165	4	40	1.0	300	40
2.300	1.192	0.165	4	48	1.0	400	40
2.350	1.416	0.139	4	16	1.1	2000	24
2.350	1.416	0.139	4	20	1.1	2000	24
2.350	1.416	0.139	4	26	1.1	1200	24
2.350	1.416	0.139	4	32	1.1	800	40
2.350	1.416	0.139	4	40	1.1	800	40
2.350	1.416	0.139	4	48	1.1	800	40
2.512	2.397	0.082	4	20	2.0	2000	24
2.512	2.397	0.082	4	32	2.0	800	40
2.512	2.397	0.082	4	40	2.0	800	40
2.512	2.397	0.082	4	48	2.0	800	40
2.635	3.596	0.055	6	40	2.0	800	40
2.635	3.596	0.055	6	48	2.0	800	40

TABLE I: Values of β , lattice sizes, temperatures, number of measurements and number of gauge copies used throughout this paper. To fix the scale we take $\sqrt{\sigma} = 440$ MeV.

For gauge fixing we employ the $Z(2)$ flip operation as has been proposed in [23]. It consists in flipping all link variables $U_{x\mu}$ attached and orthogonal to a 3d plane by multiplying them with -1 .

Such global flips are equivalent to non-periodic gauge transformations and represent an exact symmetry of the pure gauge action. The Polyakov loops in the direction of the chosen links and averaged over the 3d plane obviously change their sign. At finite temperature we apply flips only to directions $\mu = 1, 2, 3$. In the deconfinement phase, where the $Z(2)$ symmetry is restored, the $Z(2)$ sector of the Polyakov loop in the $\mu = 4$ direction has to be chosen since on large enough volumes all lattice configurations belong to the same sector, i.e. there are no flips between sectors. We choose sector with positive Polyakov loop. In the confinement phase one may use a flip in the $\mu = 4$ direction. However, in a test run we have found that at $\beta = 2.26$ studied in this paper the maximal gauge fixing functional (5) has been found in the positive Polyakov loop sector in more than 90 % cases. To save computer time we stick to this sector for all configurations at this β . Therefore, in our study the flip operations combine for each lattice field configuration the 2^3 distinct gauge orbits (or Polyakov loop

² Let us note that the 4th euclidian component $p_4 \neq 0$ has no physical meaning.

sectors) of strictly periodic gauge transformations into one larger gauge orbit.

Following Ref.[25] in what follows we call the combined algorithm employing simulated annealing (SA) algorithm (with finalizing overrelaxation) and $Z(2)$ flips the ‘FSA’ algorithm. For every configuration the Landau gauge was fixed $N_{copy} = 24(40)$ times (3(5) gauge copies for every flip-sector) on lattices with $L_s \leq 26 (L_s \geq 32)$, each time starting from a random gauge transformation of the mother configuration, obtaining in this way N_{copy} Landau-gauge fixed copies. We take the copy with maximal value of the functional (5) as our best estimator of the global maximum and denote it as best (“bc”) copy. In order to demonstrate the Gribov copy effect we compare with the results obtained from the randomly chosen first (“fc”) copy.

We present results for the unrenormalized propagators and make comments on renormalization when propagators computed at different values of β are compared or comparison with the renormalized results of other groups is necessary. Other details of our gauge fixing procedure are described in our recent papers [23–25]

To suppress ‘geometrical’ lattice artifacts, we have applied the “ α -cut” [29], i.e. $\pi k_i/L_s < \alpha$, for every component, in order to keep close to a linear behavior of the lattice momenta $p_i \approx (2\pi k_i)/(aL_s)$, $k_i \in (-L_s/2, L_s/2]$. We have chosen $\alpha = 0.5$. Obviously, this cut influences large momenta only. We did not employ the *cylinder cut* in this work.

III. GRIBOV COPY EFFECTS AND LARGE L_s BEHAVIOR OF $D_T(0)$

As has been already pointed above, the Gribov copy problem still remains acute, at least, in the deep infrared region and the choice of the efficient gauge fixing method is very important. The importance of this choice is demonstrated in Fig. 1 taken from our recent paper [25]. In this Figure we compare our bc FSA results for the bare gluon propagator $D(p)$ calculated on a 44^4 lattice with those of the standard fc OR method obtained for an 80^4 lattice and also with the fc SA results. In particular, we observe that the OR method with one gauge copy produces completely unreliable results for the range of momenta $|p| \lesssim 0.7$ GeV. (The detailed discussion can be found in [25])

Let us define the normalized difference of the fc and bc transverse propagators $\Delta_T(p)$:

$$\Delta_T(p) = \frac{D_T^{fc}(p) - D_T^{bc}(p)}{D_T^{bc}(p)}, \quad (11)$$

where the numerator has been obtained by averaging over all configurations of the difference between fc and

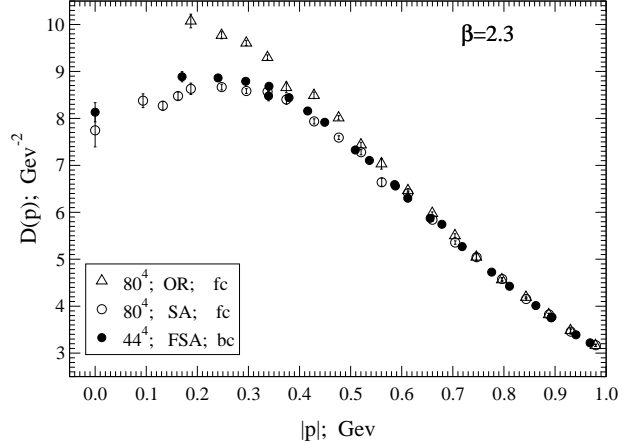


FIG. 1: Comparison of data obtained for bc FSA gauge fixing with those obtained with the standard fc OR - method and the fc SA algorithm (this Figure from paper [25])

bc transverse propagators calculated for every configuration, this average being normalized to the bc (averaged) transverse propagator. In a similar way one can define also the normalized difference of the fc and bc longitudinal propagators $\Delta_L(p)$.

The longitudinal propagators $D_L(p)$ demonstrate very weak dependence on the choice of Gribov copy. In Figure 2 we show the momentum dependence of $\Delta_L(p)$ on the 4×48^3 lattice at $\beta = 2.35, 2.512$ and $\beta = 2.26$, i.e. at temperatures both above and below transition. One can see that values of $\Delta_L(p)$ are consistent with zero for all β -values shown in the figure. This was observed on all other lattices employed in our study.

In contrast, the Gribov copy dependence of the transverse propagator is rather strong. In Figure 3 we show the momentum dependence of $\Delta_T(p)$ on various lattices at $\beta = 2.35$ ($T/T_c = 1.1$). One can see that for fixed physical momentum p the effect of Gribov copies tends to decrease with increasing volume. Such behavior is in agreement with the absence of the Gribov copies effects (within Gribov region) in the infinite volume limit, suggested by Zwanziger [30]. On the other hand, on given lattice there are always 3 or 4 minimal values of momentum for which these effects are substantial. In particular, $\Delta_T(p)$ varies between 0.35 and 0.55 for $p = 0$, between 0.09 and 0.12 for $|p| = p_{min} \equiv (2/a) \sin(\pi/L_s)$ and between 0.03 and 0.04 for momentum next after p_{min} . Similar observations were made at zero temperature as well [25].

In Figure 4 we show the parameter $\Delta_T(p)$ for two temperatures, $T/T_c = 1.1$ and $T/T_c = 2$, on lattices with approximately equal physical volumes. One can see that there is rather weak (if any) dependence of the Gribov copy effects on the temperature T .

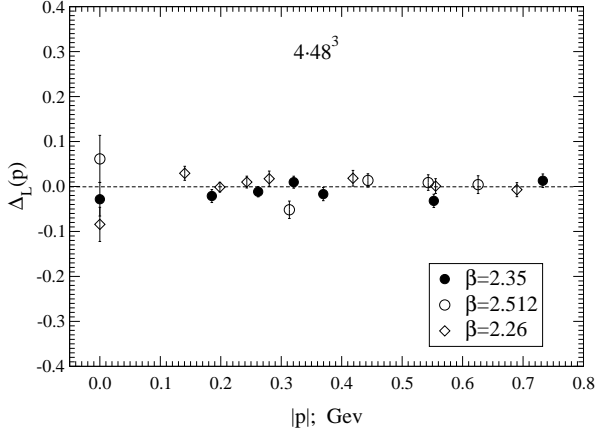


FIG. 2: The momentum dependence of $\Delta_L(p)$ for three temperatures.

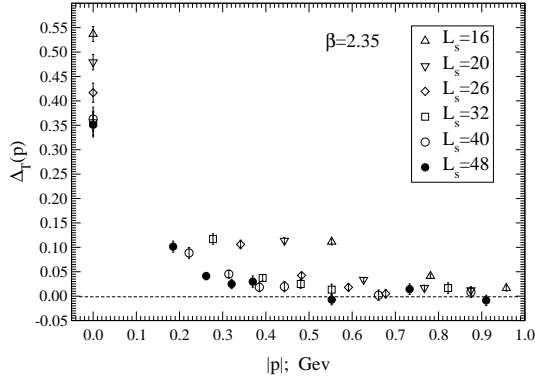


FIG. 3: The momentum dependence of $\Delta_T(p)$ at $\beta = 2.35$ on various lattices.

The comparison of the results for $\Delta_T(p)$ obtained on lattices $4 \cdot 32^3$ at $\beta = 2.512$ and 6×48^3 at $\beta = 2.635$ (both corresponding to the same temperature $T/T_c = 2$ and the same physical volume) shows that the Gribov copy effects depend weakly on the lattice spacing a .

Let us note that results for $\Delta_T(p)$ discussed above are obtained with the gauge fixing algorithm we have chosen, i.e., FSA. The value of $\Delta_T(p)$ will be essentially *higher* if one uses the OR algorithm to compute the *fc* propagator $D_T^{fc}(p)$.

In Figure 5 we show the $1/aL_s$ dependence and Gribov copy sensitivity of the zero-momentum transverse propagator $D_T(0)$ in the deconfinement phase (for $T = 1.1T_c$ and for $T = 2T_c$). The difference between *bc* values (filled symbols) and *fc* values (open symbols) is rather big, as has been already discussed above. However, with increasing size L_s the values

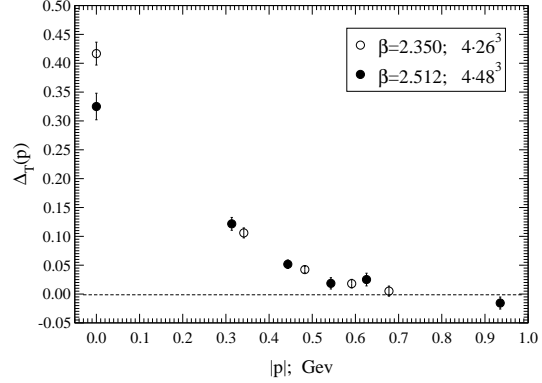


FIG. 4: The momentum dependence of $\Delta_T(p)$ on two lattices with approximately equal physical volume.

of $D_T^{bc}(0)$ and $D_T^{fc}(0)$ demonstrate a tendency to decrease; moreover, our data, especially for $T = 2T_c$, suggest that $D_T^{bc}(0)$ and $D_T^{fc}(0)$ seem to (slowly) converge in the limit $L_s \rightarrow \infty$. This convergence is again in accordance with a conjecture made by Zwanziger in [30] and in accordance with the zero-temperature case studied numerically in [22, 25].

On the other hand, our data also suggest that $D_T(0)$ is non-zero in the infinite volume limit for both values of T , in disagreement with the suggestion made in [1]. There is no indication for a vanishing transverse propagator at zero momentum for increasing volume, similarly to the situation for the zero-temperature case [22, 25]. This is in agreement with the refined Gribov-Zwanziger formalism [31, 32].

Let us note that one still cannot exclude that there are even more efficient gauge fixing methods, superior to the one we use, which could make this decreasing more drastic.

IV. VOLUME AND TEMPERATURE DEPENDENCE AND FINITE SPACING EFFECTS.

A. Volume dependence

As is well-known, the finite volume dependence is very strong near the second order phase transition point T_c . For the transverse propagator $D_T(p)$ this dependence can be seen from Figure 6 and for the longitudinal propagator $D_L(p)$ from Figure 7, both calculated at $\beta = 2.3$ (slightly above T_c) on various lattices.

Deeper inside in the deconfinement phase the finite volume effects are much less pronounced, at least at non-zero values of momentum. In Figure 8 we show the momentum dependence of the transverse propa-

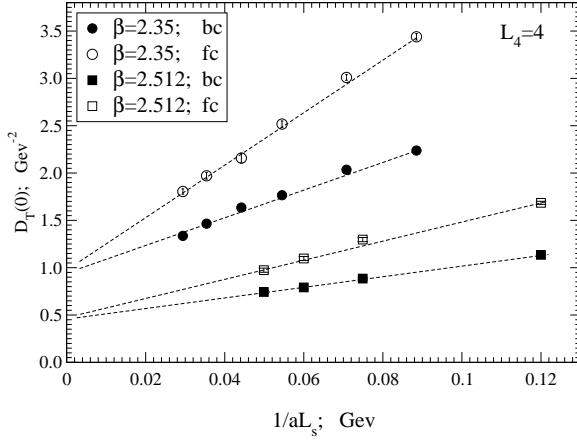


FIG. 5: The $1/aL_s$ dependence and Gribov copy sensitivity of the transverse propagator $D_T(0)$ at $\beta = 2.35$ (circles) and $\beta = 2.512$ (squares). Values of L_s are given in Table I. Filled symbols correspond to the bc ensemble, open symbols to the fc ensemble. The lines are to guide the eye.

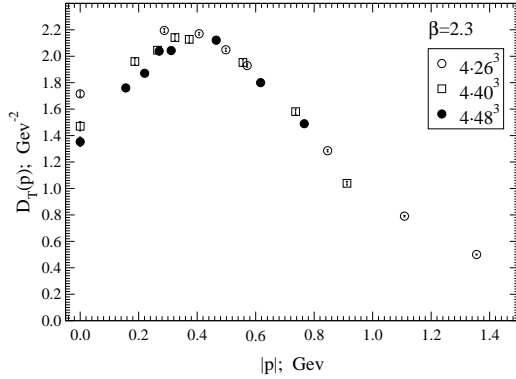


FIG. 6: The momentum dependence of the transverse propagators $D_T(p)$ on various lattices at $\beta = 2.3$.

gators $D_T(p)$ on various lattices in the deconfinement phase at $T = 1.1T_c$ and $T = 2T_c$. Apart from the strong volume dependence at $p = 0$, we see that finite volume effects are rather weak, the sizable effects are seen only for the minimal non-zero momentum p_{min} on a given lattice.

The volume dependence of the longitudinal propagators $D_L(p)$ at $T = 1.1T_c$ and at $T = 2T_c$ is presented in Figure 9. Evidently, the volume dependence of $D_L(p)$ is even weaker than that of $D_T(p)$, it is rather weak even at $p = 0$. Note that at $T = 1.1T_c$ $D_L(0)$ slowly increases with increasing volume, contrary to decreasing of $D_T(0)$.

For every lattice we observed a well-pronounced

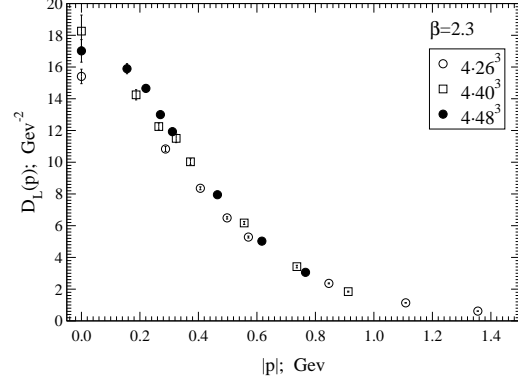


FIG. 7: The momentum dependence of the longitudinal propagators $D_L(p)$ on various lattices at $\beta = 2.3$.

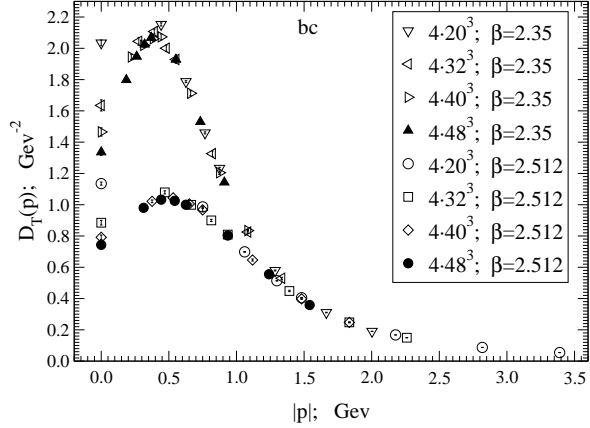


FIG. 8: The momentum and volume dependence of the transverse propagators $D_T(p)$ at $\beta = 2.35$ and $\beta = 2.512$.

maximum of the transverse propagator $D_T(p)$ at non-zero momentum p_0 with $|p_0| \sim 0.4 \div 0.5$ GeV. Deep in the deconfinement phase the maximum has been found before [10, 13, 15]. But we observed it for the first time at $T = T_c$ and $T < T_c$ as one can see in Figure 10. In our recent papers [24, 25] we reported about the existence of the maximum of the scalar propagator $D(p)$ at non-zero momentum on the symmetric lattices (zero-temperature case) when lattice size is big enough. Therefore, we conclude that the transverse propagator $D_T(p)$ has its maximum at $p_0 \neq 0$ for *all* temperatures, and the behavior of the transverse propagator in the deep infrared is not consistent with the simple pole-type behavior both in confinement and deconfinement phases.

It is instructive to compare our results for $D_T(p)$ at $T = 1.1T_c$ on $L_s = 48$ lattices with respective results of Ref. [15] obtained at this temperature on the lat-

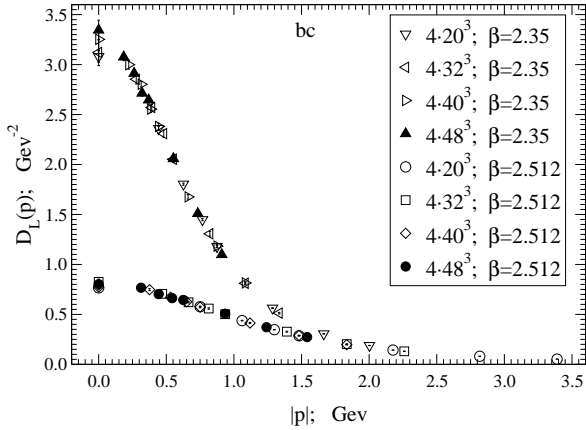


FIG. 9: The momentum dependence of the longitudinal propagators $D_L(p)$ on various lattices at $\beta = 2.35$ and $\beta = 2.512$.

tices with $L_4 = 4$ and $L_s = 46$ and presented in their Figure 1. To make this comparison we made renormalization at $\mu = 2$ GeV as it was made in [15]. In the infrared region we found both qualitative and substantial quantitative disagreement between our results and results of Ref. [15]. In particular, the clear maximum which we see in our Figure 8 at $T = 1.1T_c$ can not be seen from Figure 1 of Ref. [15]. These differences between our results and results of Ref. [15], which are just Gribov copies effects, are more essential than differences between our bc and fc results discussed in Section III.

In contrast with $D_T(p)$, the longitudinal propagator $D_L(p)$ does not show any trace of maximum at $|p| \neq 0$ both above and below T_c , as one can see in Figure 9 and Figure 11 in agreement with results of Refs. [10, 15]. This gives an idea that it can be fitted by the pole-type behavior (see Section V). The pole-type behavior at high temperature is not surprising since at high enough temperature the effective theory is the Higgs $3d$ theory with A_4 playing a role of the Higgs field.

B. Temperature dependence

The temperature dependence of the transverse propagator $D_T(p)$ near the critical point T_c is very smooth. Figure 10 makes comparison of the momentum dependence of $D_T(p)$ for three temperatures: $T = 0.9T_c$, $T = T_c$ and $T = 1.1T_c$. Indeed, there is no sign of sensitivity to the phase transition. It is worthwhile to note that the effect of renormalization do not alter this conclusion since the renormalization constants computed at $\mu = 2$ GeV differ by less than 0.5%.

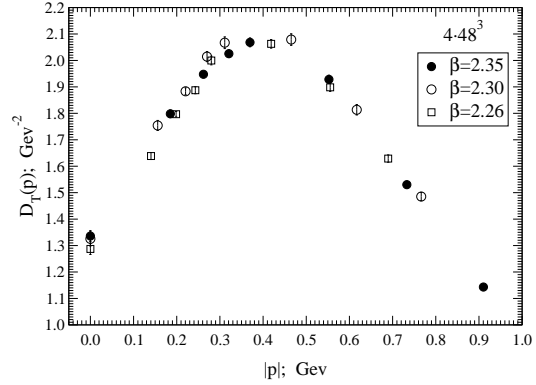


FIG. 10: The momentum dependence of the transverse propagators $D_T(p)$ near T_c on the 4×48^3 lattices.

Thus the transverse gluons in Landau gauge are not directly related to confinement [10, 33].

In contrast, the longitudinal propagator $D_L(p)$ demonstrates a drastic jump in its values in the infrared when the critical temperature is crossed from above (see Figure 11). The respective renormalization constants computed at $\mu = 2$ GeV differ by a few percent in this case and this difference has a tendency to decrease with increasing μ . The difference in the renormalization constants only slightly alters the temperature dependence of $D_L(p)$ after renormalization. Therefore, $D_L(p)$ at small momenta can be considered as an order parameter signaling the phase transition.

Note that the study of the related quantity $\Delta_{A^2} \equiv \langle g^2 A_E^2 - g^2 A_M^2 \rangle$ suggests that in the vicinity of T_c the temperature dependence of $D_L(p)$ can have rather nontrivial (non-monotonous) character [34]. Further studies at T very close to T_c are necessary to clarify this issue. Let us note also that for the first time the fast change of the longitudinal propagator near the transition point has been observed in [33] (in the $SU(3)$ case). This fast change has been recently demonstrated in Ref. [15] both in $SU(2)$ and $SU(3)$ theories.

Deep into the deconfinement phase the decreasing of the transverse propagator $D_T(p)$ at $p \sim 0$ with increasing temperature (see Figure 8) is in a qualitative agreement with dimensional reduction since according to dimensional reduction at high temperature $D_T(p)$ is to be proportional to $(g^2(T) T)^{-2}$. The quantitative agreement is not yet expected at temperatures considered here. Similarly, the electric propagator $D_L(p)$ for small momenta decreases fast with increasing temperature, see Figure 9.

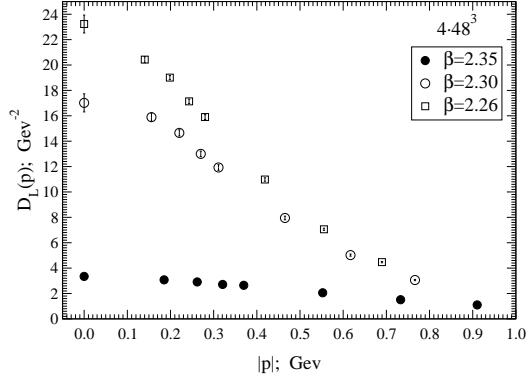


FIG. 11: The momentum dependence of the longitudinal gluon propagators $D_L(p)$ near T_c on the 4×48^3 lattices.

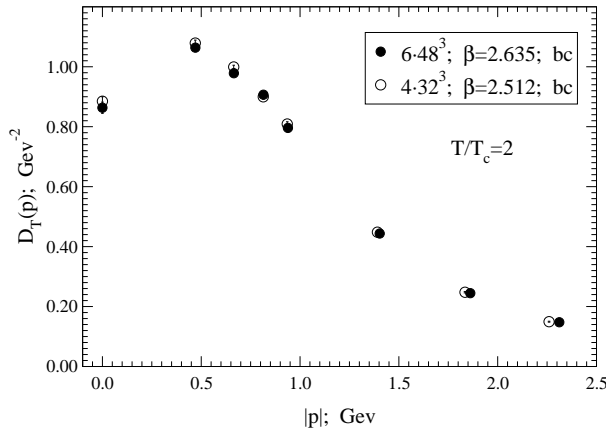


FIG. 12: The momentum dependence of the transverse propagator $D_T(p)$ on two different lattices corresponding to the same temperature and the same physical volume.

C. On the discretization errors

To estimate discretization errors at $T = 2T_c$ we calculated transverse and longitudinal propagators on two different lattices corresponding to the same physical $3d$ volume $(aL_s)^3$ but with different lattice spacing. These are lattices $L_4 = 4, L_s = 32, \beta = 2.512$ and $L_4 = 6, L_s = 48, \beta = 2.635$. In Figure 12 we show the momentum dependence of the transverse propagator $D_T(p)$ for these two lattices. One can see good agreement between results obtained on these lattices for all included momenta. This implies that at $T = 2T_c$ the discretization effects are small even on lattices with $L_4 = 4$. We expect that this is true also at higher temperatures.

Let us note that at this temperature we have employed larger L_4 -values and larger β -values (i.e.,

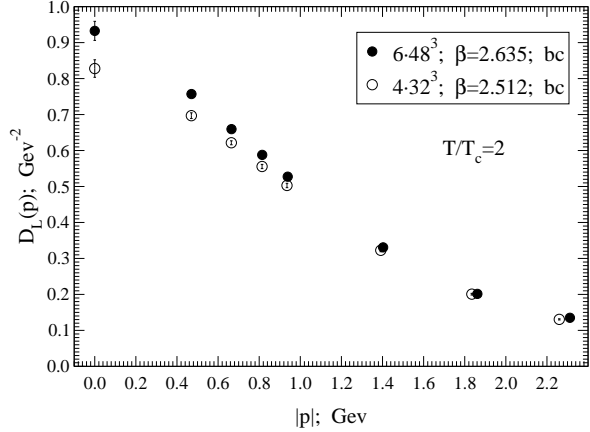


FIG. 13: The momentum dependence of the longitudinal propagator $D_L(p)$ on two different lattices corresponding to the same temperature and the same physical volume.

smaller spacings) as compared to that employed in Ref. [10]. This explains the fact that the discretization effects we find are much smaller than in that paper.

Contrary to the transverse propagator, the data for the longitudinal propagator $D_L(p)$ show substantial scaling violations in the infrared. This can be seen from Figure 13 where propagators $D_L(p)$ computed on the same lattices as used in Figure 12 are depicted. The renormalization constants computed at $\mu = 2$ GeV differ only by 4% so the scaling violations do not disappear after renormalization. Evidently, the discretization errors are large at momenta smaller than 1 GeV. To reduce the finite cut-off effects one should increase L_4 or use improved lattice action (see, e.g. [12]).

The results of our study of the scaling behavior at zero temperature [25] suggest that for smaller values of β (i.e., $\beta = 2.35$, $\beta = 2.3$ and $\beta = 2.26$) discretization errors are substantial for both propagators.

V. ON THE SCREENING MASSES

One of the interesting features of the high temperature phase is the appearance of the infrared mass scale parameters : m_E ('electric') and m_M ('magnetic'). These parameters (or 'screening masses') define screening of electric and magnetic fields at large distances and, therefore, control the infrared behavior of $D_L(p)$ and $D_T(p)$. The electric screening mass m_E has been computed in the leading order of perturbation theory long ago: $m_E^2 = \frac{2}{3}g^2T^2$ for $SU(2)$ gluodynamics. But at the next order the problem of the infrared divergencies has been found. On the other hand, the magnetic mass m_M is entirely nonperturba-

tive in nature. Thus a first-principles nonperturbative calculations in lattice QCD should play an important role in the determination of these quantities.

As has been already mentioned above, the momentum dependence of the longitudinal propagator $D_L(p)$ in the deep infrared is expected to fit the pole-type behavior. Indeed, as an illustration, in Figure 14 we show the momentum dependence of the inverse propagator $D_L^{-1}(p)$ at $T = 0.9T_c$ and $T = 1.1T_c$. Since the volume effects are small enough, at least, at $p \neq 0$, we use data obtained on all lattices listed in Table I with exception for $p = 0$. For this momentum we included data for the largest lattice only.

One can see that at small momenta the dependence on p^2 is linear. Thus in the infrared region we have used the fitting formula

$$D_L^{-1}(p) = A \cdot (p^2 + m_E^2). \quad (12)$$

The results of the fits are presented in the Table II. At $T = 2T_c$ we can compare our results with results of Ref.[12] shown in their Figure 3. We find that m_E computed on lattices with $L_4 = 4$ is in good agreement with respective result of Ref.[12]. For finer lattice spacing ($L_4 = 6$) our value is only slightly smaller than the value for $L_4 = 4$ (see Table II) indicating small scaling deviations, while in Ref.[12] the value obtained on the lattice with $L_4 = 8$ was substantially higher. We believe that due to simplicity of the fitting function (12) extracting of m_E from $D_L(p)$ allows more precise measurement of this quantity than its determination from the correlator $D_E(z)$ used in Ref.[12].

In Table II we also show the maximal momenta p_{max} included into a fit. This value was defined by condition that the χ^2/dof value for the fit was smaller than 2. One can see that p_{max} increases with T .

β	T/T_c	$m_E[\text{Gev}]$	m_E/T	$p_{max}^2[\text{GeV}^2]$
2.260	0.9	0.41(1)	1.53(4)	0.15
2.300	1.0	0.46(1)	1.54(4)	0.10
2.350	1.1	0.73(2)	2.06(6)	0.30
2.512	2.0	1.21(2)	2.02(4)	1.0
2.635	2.0	1.15(3)	1.92(6)	1.0

TABLE II: Values of the screening mass m_E obtained from fits to eq.(12) and maximal momenta used in the fit p_{max} .

In contrast, the transverse propagator $D_T(p)$ has a form which is not compatible with the simple pole-type behavior, so for m_M another, different from pole mass, definition is necessary. We applied two fitting functions to our data for $D_T(p)$. One of them, Gaussian function with shifted argument

$$f_G(p) = C e^{-(|p| - |p_0|)^2 / m_M^2} \quad (13)$$

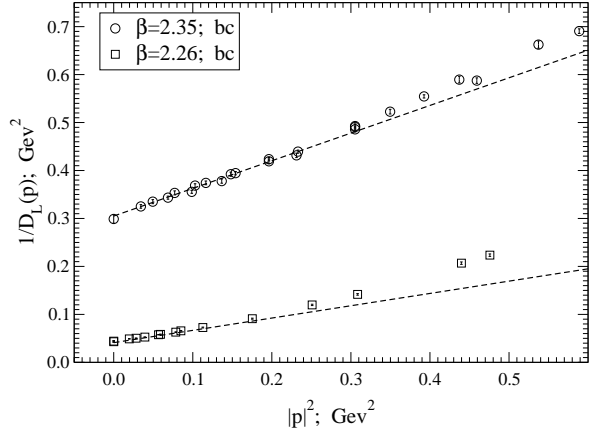


FIG. 14: The momentum dependence of the inverse longitudinal propagator $1/D_L(p)$ at $\beta = 2.35$ and $\beta = 2.26$.

has been used recently in Ref. [25] to fit the $T = 0$ gluon propagator in the infrared region of momenta. In (13) m_M is a massive parameter, $|p_0|$ is momentum shift and C a normalization constant. Another fitting function is shifted pole propagator of the form

$$f_P(p) = \frac{C}{(m_M^2 + (|p| - |p_0|)^2)} \quad (14)$$

(we keep same notations for fitting parameters). The zero momentum was excluded from the fitting range, the maximal momentum was determined by requirement that respective χ^2/N_{dof} was smaller than 1. We found that both fits work well in the infrared with better performance (larger range) for the fit function (14).

β	T/T_c	$m_M[\text{Gev}]$	m_M/T	$p_{max}[\text{GeV}]$	$ p_0 [\text{Gev}]$
2.350	1.1	0.56(1)(4)	1.59(3)(12)	1.3	0.40(1)
2.512	2.0	0.78(1)(7)	1.30(2)(11)	1.3	0.51(1)

TABLE III: Values of the mass parameter m_M obtained from fits to eq.(14) and maximal momenta used in the fit p_{max} .

In Table III we show fitting parameters for fit function eq. (14). The second error for m_M is the difference from result for fit to eq. (13) in which case m_M was bigger. The difference in values of $|p_0|$ for two fits was less than 1%.

We can compare our value for m_M at $T/T_c = 2$ with result from Ref.[12] presented in Figure 4. In that paper result for $T/T_c = 2$ was obtained on $32^2 \times 64 \times 8$ lattice. They found $m_M/T = 2.0(3)$, i.e. much higher than our value. Apart from difference in the

definition of m_M this deviation might be explained by the Gribov copy effect, which is much stronger for m_M than for m_E . We need to make computations at higher temperatures to make more detailed comparison with results of Ref.[12].

VI. CONCLUSIONS

In this work we studied numerically the behavior of the Landau gauge longitudinal and transverse gluon propagators in pure gauge $SU(2)$ lattice theory in the infrared region of momentum values. The special accent has been made on the study of the dependence of these 'observables' on the choice of Gribov copies.

The simulations have been performed using the standard Wilson action at temperatures from $0.9T_c$ up to $2T_c$ on lattices with $L_4 = 4$ and spatial linear sizes up to $L = 48$. For $T = 2T_c$ simulations were repeated on lattices with $L_4 = 6$. For gauge fixing gauge orbits enlarged by $Z(2)$ flip operations were considered with up to 5 gauge copies in every flip-sector (in total, up to 40 gauge copies). The maximization of the gauge functional was achieved by the simulated annealing method always combined with consecutive overrelaxation.

Our findings can be summarized as follows.

Similarly to the gluon propagator at $T = 0$, the Gribov copy dependence of the transverse propagators $D_T(p)$ is *very strong* in the infrared, more precisely, at a few minimal (for given lattice) momenta. At the same time for fixed physical momentum p the effect of Gribov copies decreases with increasing volume in agreement with [30]. We found no dependence of the Gribov copies effects on the temperature or lattice spacing.

The Gribov copy dependence of the longitudinal propagators $D_L(p)$ is very weak, at least, at non-zero momenta, and is comparable with the statistical errors (so called 'Gribov noise').

We have to emphasize that our conclusions for Gribov copies effects are relevant for our gauge fixing algorithm and they might change if another, less efficient, algorithm is used.

With increasing size L_s the bc -values of $D_T(0)$ and fc -values of $D_T(0)$ demonstrate a tendency to decrease; moreover, $D_T^{bc}(0)$ and $D_T^{fc}(0)$ seem to (slowly) converge in the limit $L_s \rightarrow \infty$ which is in accordance with a conjecture made by Zwanziger in [30] and in accordance with the zero-temperature case studied numerically in [22, 25]. However, $D_T(0)$ is *non-zero* in the infinite volume limit, in disagreement with the suggestion made in [1].

We observed the existence of the maximum of the $D_T(p)$ at momenta $|p| \sim 0.4 \div 0.5$ GeV *not only* in

the deconfinement phase but also for $T \leq T_c$. Thus we confirmed that there is *no* possibility to explain the IR-behavior of the transverse $D_T(p)$ gluon propagator on the basis of a simple pole-type behavior $\sim 1/(p^2 + m^2)$. Instead we fitted this propagator to fitting functions eq.(13) and eq.(14) with massive parameter m_M . m_M/T is slowly decreasing with increasing temperature. To check if this decreasing is compatible with gT behavior, as expected for the magnetic screening mass, as well as to compare our results for this parameter with results for magnetic screening mass, obtained by other authors, we need to repeat our computations at higher temperatures.

For $D_L(p)$ we found good agreement with 'pole-like' behavior at small enough momenta $p < p_{max}$ with p_{max} increasing with T . Our value for m_E at $T = 2T_c$ agrees well with result from [12] obtained also on lattices with $L_4 = 4$. Again, we need results at higher temperatures to compare with other results and with the perturbation theory predictions. We shall note that our method of computing m_E in the momentum space rather than in the coordinate space gives rise to higher precision.

Away from the transition temperature the longitudinal propagators $D_L(p)$ demonstrate very weak volume dependence. The volume dependence of the transverse propagators $D_T(p)$ is strong at $p = 0$ and it is weak at $p > 0$.

We found very small scaling violations for $D_T(p)$ at $T = 2T_c$ comparing results obtained on lattices with $L_4 = 4$ and 6. In opposite, for $D_L(p)$ scaling violations in the infrared are substantial.

We confirmed the observation made in Ref. [15] that the longitudinal propagator $D_L(p)$ in the infrared increases fast when temperature crosses transition from above. From results presented in Ref. [15] for $T < T_c$ it is clear that $D_L(p)$ has a maximum near to T_c . This is also in agreement with findings for $\Delta_{A^2} \equiv \langle g^2 A_E^2 - g^2 A_M^2 \rangle$ [34].

Acknowledgments

This investigation has been partly supported by the Heisenberg-Landau program of collaboration between the Bogoliubov Laboratory of Theoretical Physics of the Joint Institute for Nuclear Research Dubna (Russia) and German institutes, partly by the Federal Special-Purpose Programme 'Cadres' of the Russian Ministry of Science and Education and partly by the grant for scientific schools NSh-6260.2010.2. VB is supported by grants RFBR 09-02-00338-a and RFBR 08-02-00661-a.

-
- [1] I. Zahed and D. Zwanziger, Phys. Rev. **D61**, 037501 (2000), hep-th/9905109.
 - [2] M. Gyulassy and L. McLerran, Nucl. Phys. **A750**, 30 (2005), nucl-th/0405013.
 - [3] R. Baier, Y. L. Dokshitzer, A. H. Mueller, S. Peigne, and D. Schiff, Nucl. Phys. **B483**, 291 (1997), hep-ph/9607355.
 - [4] R. Baier, Y. L. Dokshitzer, A. H. Mueller, S. Peigne, and D. Schiff, Nucl. Phys. **B484**, 265 (1997), hep-ph/9608322.
 - [5] M. Gyulassy, I. Vitev, X.-N. Wang, and B.-W. Zhang (2003), nucl-th/0302077.
 - [6] A. Kovner and U. A. Wiedemann (2003), hep-ph/0304151.
 - [7] X.-N. Wang, Phys. Lett. **B485**, 157 (2000), nucl-th/0003033.
 - [8] A. Maas, J. Wambach, and R. Alkofer, Eur. Phys. J. **C42**, 93 (2005), hep-ph/0504019.
 - [9] A. Maas, Mod. Phys. Lett. **A20**, 1797 (2005), hep-ph/0506066.
 - [10] A. Cucchieri, A. Maas, and T. Mendes, Phys. Rev. **D75**, 076003 (2007), hep-lat/0702022.
 - [11] U. M. Heller, F. Karsch, and J. Rank, Phys. Lett. **B355**, 511 (1995), hep-lat/9505016.
 - [12] U. M. Heller, F. Karsch, and J. Rank, Phys. Rev. **D57**, 1438 (1998), hep-lat/9710033.
 - [13] A. Cucchieri, F. Karsch, and P. Petreczky, Phys. Rev. **D64**, 036001 (2001), hep-lat/0103009.
 - [14] A. Cucchieri and T. Mendes, PoS **LAT2007**, 297 (2007), 0710.0412.
 - [15] C. S. Fischer, A. Maas, and J. A. Mueller (2010), 1003.1960.
 - [16] C. Parrinello and G. Jona-Lasinio, Phys. Lett. **B251**, 175 (1990).
 - [17] D. Zwanziger, Nucl. Phys. **B345**, 461 (1990).
 - [18] A. Nakamura and M. Plewnia, Phys. Lett. **B255**, 274 (1991).
 - [19] V. G. Bornyakov, V. K. Mitrjushkin, M. Müller-Preussker, and F. Pahl, Phys. Lett. **B317**, 596 (1993), hep-lat/9307010.
 - [20] V. K. Mitrjushkin, Phys. Lett. **B389**, 713 (1996), hep-lat/9607069.
 - [21] T. D. Bakeev, E. M. Ilgenfritz, V. K. Mitrjushkin, and M. Müller-Preussker, Phys. Rev. **D69**, 074507 (2004), hep-lat/0311041.
 - [22] I. L. Bogolubsky, G. Burgio, V. K. Mitrjushkin, and M. Müller-Preussker, Phys. Rev. **D74**, 034503 (2006), hep-lat/0511056.
 - [23] I. L. Bogolubsky, V. G. Bornyakov, G. Burgio, E.-M. Ilgenfritz, V. K. Mitrjushkin, and M. Müller-Preussker, Phys. Rev. **D77**, 014504 (2008), 0707.3611.
 - [24] V. G. Bornyakov, V. K. Mitrjushkin, and M. Müller-Preussker, Phys. Rev. **D79**, 074504 (2009), 0812.2761.
 - [25] V. G. Bornyakov, V. K. Mitrjushkin, and M. Müller-Preussker, Phys. Rev. **D81**, 054503 (2010), 0912.4475.
 - [26] P. Boucaud et al., Phys. Rev. **D82**, 054007 (2010), 1004.4135.
 - [27] J. E. Mandula and M. Ogilvie, Phys. Lett. **B185**, 127 (1987).
 - [28] J. I. Kapusta, Cambridge University Press, New York, NY p. 70 (1979).
 - [29] Y. Nakagawa et al., Phys. Rev. **D79**, 114504 (2009), 0902.4321.
 - [30] D. Zwanziger, Phys. Rev. **D69**, 016002 (2004), hep-ph/0303028.
 - [31] D. Dudal, S. P. Sorella, N. Vandersickel, and H. Verschelde, Phys. Rev. **D77**, 071501 (2008), 0711.4496.
 - [32] D. Dudal, J. A. Gracey, S. P. Sorella, N. Vandersickel, and H. Verschelde, Phys. Rev. **D78**, 065047 (2008), 0806.4348.
 - [33] J. E. Mandula and M. Ogilvie, Phys. Lett. **B201**, 117 (1988).
 - [34] M. N. Chernodub and E. M. Ilgenfritz, Phys. Rev. **D78**, 034036 (2008), 0805.3714.